Digital Microfluidics

Kihwan Choi,[1,3] Alphonsus H.C. Ng,[2,3] Ryan Fobel,[2,3] and Aaron R. Wheeler[1,2,3]

[1]Department of Chemistry, University of Toronto, Toronto, Ontario M5S 3H6, Canada

[2]Institute for Biomaterials and Biomedical Engineering, University of Toronto, Toronto, Ontario M5S 3G9, Canada

[3]The Terrence Donnelly Center for Cellular and Biomolecular Research, Toronto, Ontario M5S 3E1, Canada; email: aaron.wheeler@utoronto.ca

Annu. Rev. Anal. Chem. 2012. 5:413–40

First published online as a Review in Advance on April 9, 2012

The *Annual Review of Analytical Chemistry* is online at anchem.annualreviews.org

This article's doi: 10.1146/annurev-anchem-062011-143028

1936-1327/12/0719-0413$20.00

Keywords

droplet, electrowetting on dielectric, dielectrophoresis, diagnosis, proteomics, bioanalysis

Abstract

Digital microfluidics (DMF) is an emerging liquid-handling technology that enables individual control over droplets on an open array of electrodes. These picoliter- to microliter-sized droplets, each serving as an isolated vessel for chemical processes, can be made to move, merge, split, and dispense from reservoirs. Because of its unique advantages, including simple instrumentation, flexible device geometry, and easy coupling with other technologies, DMF is being applied to a wide range of fields. In this review, we summarize the state of the art of DMF technology from the perspective of analytical chemistry in sections describing the theory of droplet actuation, device fabrication and integration, and applications.

1. INTRODUCTION

Digital microfluidics (DMF) is an emerging liquid-handling technology that manipulates liquids in discrete droplets in integrated microfluidic devices (1–7). There are some disagreements about nomenclature, but here we use the term DMF to refer to integrated systems in which droplets are manipulated on an array of electrodes, rather than systems in which droplets are manipulated in enclosed microchannels. The latter format is a popular and useful paradigm in microfluidics and has been reviewed extensively elsewhere (8–10); in this review, we focus on the former type of system.

In DMF, picoliter- to microliter-sized droplets are independently addressed on an open array of electrodes coated with a hydrophobic insulator. Through the application of a series of potentials to these electrodes, droplets can be individually made to merge, mix, split, and dispense from reservoirs (**Figure 1*a***). Like the more common channel-based microfluidic format, DMF enjoys the benefits of low reagent consumption and fast heat transfer, and it can be easily integrated with other analytical techniques. However, DMF possesses salient features that are not present in channel-based microfluidics. In DMF, each droplet is controlled individually without the need for networks of channels, pumps, valves, or mechanical mixers. Thus, various processes can be performed simultaneously with a simple and compact design. Because droplets are manipulated on generic arrays of electrodes, droplet operations are reconfigurable from experiment to experiment. It is also straightforward to collect samples after processing for preparative applications, because droplet volumes are relatively large and DMF devices are often open to atmosphere. In addition, solid samples in DMF systems can be handled and used without the risk of clogging. In this review, we summarize the state of the art of DMF technology from the perspective of analytical chemistry in sections describing the theory of droplet motion, fabrication and integration, and applications. The last section may be the most interesting, given that DMF is proving useful for a remarkably broad range of applications in analytical chemistry and beyond.

2. THEORY OF DIGITAL MICROFLUIDICS

Figure 1*b* depicts two common configurations of DMF devices: single-plate (also referred to as open) (11), and two-plate (closed) (12–14) devices. In the two-plate format, droplets are sandwiched between two substrates patterned with electrodes. Typically, the top plate consists of a continuous ground electrode formed by a transparent, conductive indium tin oxide (ITO) layer. The bottom plate houses an array of actuation electrodes. In the one-plate format, droplets sit on a single substrate bearing both actuation and ground electrodes. In both cases, an insulating dielectric layer covers the bottom-plate electrodes, and all surfaces are covered by a hydrophobic coating. Two-plate devices are often operated in air, although substitution with other filler media, such as

Figure 1

Digital microfluidics (DMF). (*a*) Droplet operations in DMF, including mixing, splitting, merging, and dispensing from reservoirs. (*b*) Side-view schematics of two-plate and one-plate DMF devices. The two-plate device schematic includes an overlaid circuit model. A top-view schematic of the two-plate device is shown below the side-view schematic. The circuit parameters depend on the cross-sectional area of the droplet overlapping with the activated (*red*) electrode: $A = xL$. (*c*) Driving force estimation for a two-plate DMF device operating on phosphate-buffered saline (PBS), deionized (DI) water, toluene, and methanol. Forces are based on an electrode size of 1 mm^2, 6 μm of Parylene C as a dielectric, 235 nm of Teflon® AF as a hydrophobic layer, an interplate spacing of 150 μm, and an applied voltage of 100 V_{rms} for a range of frequencies (100 Hz to 1 MHz).

silicone oil, can reduce the voltage necessary for droplet movement (13). Although the operational principles are similar, two-plate devices enable a wider range of operations, including dispensing, moving, splitting, and merging (13, 14). One-plate devices are incapable of splitting and dispensing, but they are well suited for preparative applications in which analytes are recovered after droplet actuation.

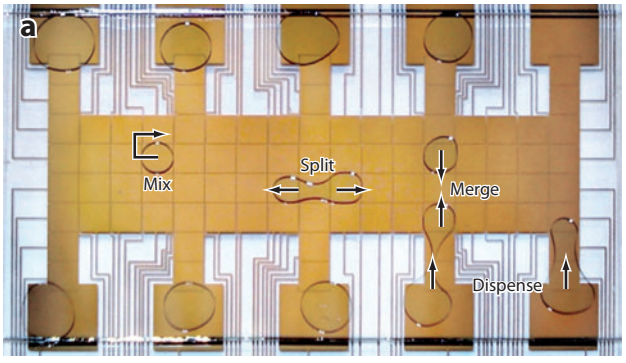

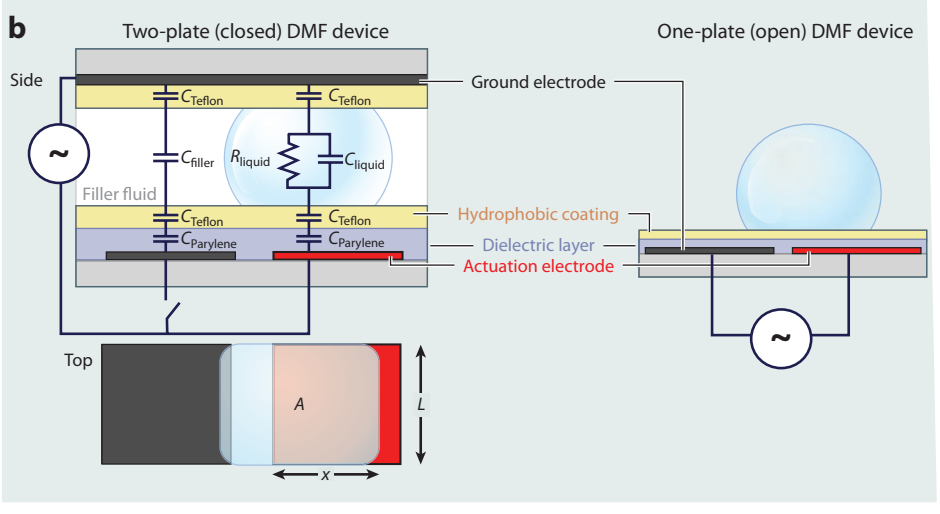

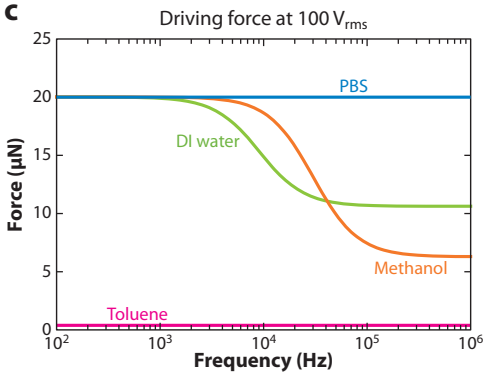

Forces that affect droplet movement can be divided into driving and resistive forces. Theoretical methods for estimating the driving forces have been reported by several groups. Early attempts were based on a thermodynamic approach using the Young-Lippman equation (13–15),

$$\cos\theta = \cos\theta_0 + \frac{\varepsilon_0 \varepsilon_r V^2}{2\gamma d}, \tag{1}$$

where θ and θ_0 are the static contact angles with and without applied voltage, respectively; ε_r is the relative permittivity of the dielectric; ε_0 is the permittivity of free space; V is the applied voltage; γ is the liquid/filler media surface tension; and d is the dielectric thickness. In this approach, droplet movement was assumed to occur because of capillary pressure that results from asymmetric contact angles across the droplet. The driving force, F, can be derived from (15)

$$L\gamma\,(\cos\theta - \cos\theta_0) = \frac{\varepsilon_0 \varepsilon_r L V^2}{2d}, \tag{2}$$

where L is the length of the contact line overlapping the actuated electrode. This approach is based on experiments on sessile droplets and a phenomenon termed electrowetting on dielectric (EWOD) (16, 17), which has led to numerous references in the literature to an EWOD-based force (13–15). Note that the driving force in DMF is a result of electrostatic forces and that a large contact angle change is not a requirement for droplet movement; instead, the wetting is an observable effect of the forces acting on the droplet (18–22). The thermodynamic (or EWOD) approach requires knowledge of the advancing and receding contact angles and/or estimation of these values on the basis of the Young-Lippman equation. This approach also fails to explain the liquid-dielectrophoretic force, which is predominant at high frequencies and/or for dielectric liquids (18–20).

A more direct and generalized approach for estimating the force on a droplet uses a circuit representation of the DMF device (**Figure 1*b***) and either the Maxwell stress tensor (18–20) or the electromechanical framework (21). Following the electromechanical derivation, the amount of energy, E, capacitively stored in the system is calculated as a function of frequency and droplet position along the x axis (the direction of droplet propagation), assuming that the cross-sectional area of the drop can be approximated as a square with sides of length L (21):

$$E(f,x) = \frac{L}{2}\left(x\sum_i \frac{\varepsilon_0 \varepsilon_{ri,\text{liquid}} V_{i,\text{liquid}}^2 (j2\pi f)}{d_i} + (L-x)\sum_i \frac{\varepsilon_0 \varepsilon_{ri,\text{filler}} V_{i,\text{filler}}^2 (j2\pi f)}{d_i}\right), \tag{3}$$

where $\varepsilon_{ri,\text{liquid}}$, $V_{i,\text{liquid}}$ and $\varepsilon_{ri,\text{filler}}$, $V_{i,\text{filler}}$ are the relative permittivity and voltage drop for the liquid and filler fluid portions of the electrode, respectively; and d_i is the thickness of layer i. The i subscript represents one of the dielectric, top and bottom hydrophobic, and liquid/filler layers. The change in energy as x goes from zero to L is equivalent to the work done on the system; therefore, differentiating Equation 3 with respect to x yields the driving force as a function of frequency:

$$F(f) = \frac{\partial E(f,x)}{\partial x} = \frac{L}{2}\left(\sum_i \frac{\varepsilon_0 \varepsilon_{ri,\text{liquid}} V_{i,\text{liquid}}^2 (j2\pi f)}{d_i} - \sum_i \frac{\varepsilon_0 \varepsilon_{ri,\text{filler}} V_{i,\text{filler}}^2 (j2\pi f)}{d_i}\right). \tag{4}$$

A critical frequency, f_c, can be calculated for each device geometry/liquid combination (21). Below this frequency, the estimated force reduces to that predicted by the thermodynamic (or EWOD) method. In this regime, the force acting on the droplet arises from charges accumulated near the three-phase contact line being electrostatically pulled toward the actuated electrode, and its magnitude depends almost exclusively on the capacitive energy stored in the dielectric layer. Above the critical frequency, a significant electric field gradient is established within the droplet,

which causes a liquid-dielectrophoretic force to pull the droplet toward the activated electrode. In this case, the force is weighted by the difference in permittivity between the liquid and the filler medium. For a dielectric liquid in an aqueous filler media, negative dielectrophoresis can be used to push the droplet away from an actuated electrode (23). **Figure 1*c*** provides force estimates for some common lab reagents obtained with typical device parameters. At low frequencies (below ~10 kHz), forces on the order of tens of micronewtons can be applied to a wide range of fluids by use of a driving voltage of 100 V_{rms}. Moving liquids that have both low conductivity and low permittivity can require prohibitively high voltages even at dc (24), although this situation can sometimes be ameliorated by mixing in a second liquid to adjust the overall electrical properties.

In addition to the driving electrostatic force acting on the drop, there exists (*a*) a shear force between the drop and the plates (15, 25) and (*b*) a viscous drag force resulting from displacement of the filler fluid (25); both of these factors impede drop motion. The shear force results in a threshold voltage, V_{min}, that must be applied to initiate drop displacement. Although Equation 4 predicts an actuation force that scales with the square of the applied voltage, this relationship breaks down at what is commonly referred to as the voltage saturation limit. The mechanism underlying saturation is still the subject of debate, although it is thought to be linked to the contact angle saturation reported in the electrowetting literature (15, 26). Possible explanations include gas ionization at the contact line (27), charge trapping in the dielectric layer (28), ejection of satellite microdroplets (29), and a zero solid-liquid interface tension limit at the contact line (26).

3. DEVICE DESIGN AND IMPLEMENTATION

A wide range of fabrication methods, droplet actuation schemes, and analytical techniques have been developed in DMF to meet the needs of different applications. In this section, we discuss the capabilities and limitations of these developments.

3.1. Fabrication

Standard DMF devices comprise four key components: substrates, electrodes, a dielectric layer, and hydrophobic layers. The proper choice of device substrate material is important, as it determines the fabrication process and influences the allowable geometries. Glass and silicon have been widely used as substrates because of their chemical inertness. The main drawbacks of glass and silicon devices are throughput and cost. There is a current trend toward use of printed circuit board (PCB) substrates because of their low cost and batch fabrication (30). Moreover, the complicated wiring between pads and electrodes that is typical for single-layer glass devices can be avoided through the use of the multilayer format of PCB substrates (31, 32). In addition, flexible devices can be formed from PCB substrates (33). DMF electrodes are formed from metals (e.g., chromium, aluminum, gold, copper) or other conductive materials (e.g., ITO, doped polysilicon). An insulating dielectric layer is deposited onto the electrodes, which facilitates the buildup of charges or field gradients for droplet actuation (see Section 2, above). The dielectric layer can be formed with various techniques, including vapor deposition (Parylene, amorphous fluoropolymers, and silicon nitride), thermal growth (silicon oxide), and spin-coating [polydimethylsiloxane (PDMS) or SU-8]. Finally, a hydrophobic coating, typically a fluoropolymer such as Teflon® AF, is used to reduce the surface energy for actuation of aqueous droplets.

Photolithography and wet or dry etching (typically performed in a clean room) are the most common techniques used in fabricating DMF devices. However, these methods are not accessible to all users, which has led to the development of numerous alternatives. For example,

Watson et al. (34) reported three microcontact printing techniques for forming DMF devices outside of the clean room. The most robust of these methods used a PDMS stamp to transfer a pattern of 1-hexadecanethiol onto a gold surface to protect the covered regions from gold etchant. The stamp is reusable (and pattern transfer onto the gold does not require a clean room), but a photolithography step (typically in a clean room) is required to form the stamp. A second method relies on pattern transfer with a desktop laser printer (35). Device designs are printed directly onto a copper-clad sheet of polyimide, and the laser toner serves as a mask for copper etching. This method is fast and elegant, but the resolution and printing quality of the laser printer are limiting factors. A third technique uses a mask drawn with a permanent marker (36). After an outline of an electrode array is drawn on the surface of a substrate, gaps between the electrodes are formed with a razor. This process is carried out by hand without any instrumentation. In an attempt to make the technique even more widely accessible, the authors of this study (36) demonstrated the use of inexpensive food wrap and water repellants as dielectric and hydrophobic coatings, respectively. These and other non–clean room methods are becoming popular for use in fabricating devices for various applications (37).

3.2. Droplet Actuation

In standard DMF platforms, droplets are actuated in digital microfluidic systems through the application of electrical potentials between pairs of electrodes (Section 2). Devices are configured such that the droplets are surrounded by air or oil. Compared with actuation in air, oil-immersed systems are compatible with lower voltages for droplet actuation and droplet evaporation is eliminated. Disadvantages of oil-filled systems include analyte partitioning into oil, oil leakage from the device, incompatibility with oil-miscible liquids, and incompatibility with applications relying on droplet drying. A hybrid technique combining elements of both oil and air immersion is the use of core-shell systems, in which aqueous droplets are encapsulated in droplets of oil and actuated in a device that is filled with air (38, 39).

Although DMF systems are usually powered through the application of electrical fields to a pattern of electrodes (as described in Section 2), many variations on this scheme have been demonstrated. For example, there are systems that rely on optical forces (40–44), magnetic forces (45, 46), thermocapillary forces (47, 48), and surface acoustic waves (SAWs) (49). For systems powered by optical forces (40–44), devices bearing a photoconductive layer are formed; when exposed to a pattern of light, the impedance of the exposed area is reduced (forming a virtual electrode). Compared with actuation on standard devices with physical electrodes, optically driven systems are advantageous in that complex wiring and interconnection problems can be avoided. Moreover, one can tune the size of the droplets by varying the size of the pattern of light. The technique has recently become more accessible with the introduction of droplet manipulation through a liquid crystal display (**Figure 2*a***) (44). For systems powered by magnetic forces (45, 46), droplets containing magnetic particles are actuated through the movement of magnets underneath a flat substrate (**Figure 2*b***). Like techniques relying on light, this method is advantageous in that an array of electrodes is not necessary; however, all droplets must contain magnetic particles. In systems powered by thermocapillary forces (47, 48), droplets are actuated through the application of temperature gradients generated with thin-film resistive heaters on a flat substrate (**Figure 2*c***). Relative to the other techniques, thermocapillary forces do not (as yet) provide fine control over droplet position, and in addition, the temperature changes may be problematic, depending on the application. Finally, in systems powered by SAW forces (49), a SAW generated by a high-frequency power source is propagated onto a droplet, which causes the droplet to move (**Figure 2*d***). In addition, a SAW can be used to agitate an otherwise stationary droplet,

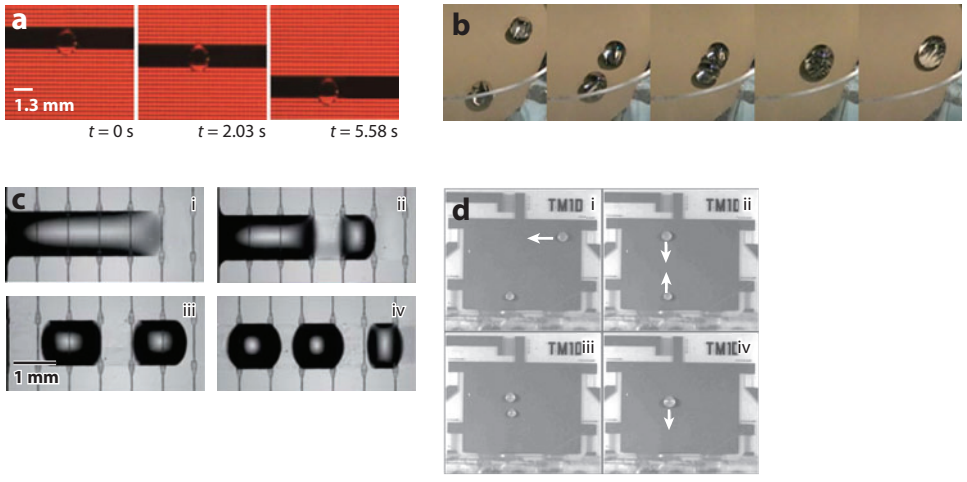

Figure 2

Electrode-less actuation modalities of digital microfluidics. (*a*) Droplet movement to the top of a liquid crystal display by optical forces. Reproduced from Reference 44 with permission from the Royal Society of Chemistry. (*b*) Merging of droplets with magnetic forces. Reprinted from Reference 46 with permission from Elsevier. (*c*) Splitting of a droplet through thermocapillary actuation. Reproduced from Reference 48 with permission from the Royal Society of Chemistry. (*d*) Droplet movement (*arrows*) driven by surface acoustic-wave forces. Reproduced from Reference 49 with permission from the Royal Society of Chemistry.

facilitating rapid mixing and enhanced reaction rates. A disadvantage of such techniques is the need for piezoelectric substrates.

In DMF systems, surface flaws such as scratches, dust, and reagents that have adsorbed onto the surface can cause droplets to resist movement or to fail to move. This phenomenon can be overcome by implementing a droplet-sensing and feedback control system such that when droplet movement failure is observed, additional driving pulses can be applied until the droplet completes the desired application. Because standard configurations of DMF involve droplets sandwiched between two electrodes (**Figure 1**), a convenient parameter for sensing droplet position is to measure the capacitance change associated with droplet movement. Ren et al. (50) implemented a ring oscillator circuit to sense the impedance of droplets on DMF systems. This system was coupled with an off-chip pressure source and was used to control the accumulation of fluid on an activated electrode until the impedance reached a designated cutoff value. This development was a useful step forward (and resulted in better precision for droplet dispensing), but the requirement of an off-chip pump is not ideal. Gong & Kim (31) introduced a feedback technique that uses an electronic circuit (with no off-chip pressure source). A proportional integral derivative control algorithm was used to facilitate high-precision droplet dispensing; the coefficients of variation (CVs) of droplet volumes were as low as 1%. In addition, different volumes of droplets were generated with fixed electrode size. However, this technique requires complicated electronic circuits for impedance measurements and dc voltages to drive droplets (dc driving voltages are often avoided in DMF, as they can result in unwanted electrolysis). Shih et al. (51) recently introduced a simple feedback control system compatible with ac driving voltages by using a circuit comprising only a few resistors and a capacitor. This sensing system was useful for implementing a feedback control system for high-fidelity actuation of sticky solutions containing proteins that are problematic for non–feedback controlled systems.

Protein adsorption to the hydrophobic surface of DMF devices hinders droplet actuation. Because many applications involve solutions of proteins or other hydrophobic molecules, biofouling is a serious obstacle. Several strategies have been developed to overcome this problem. The first strategy is to use water-immiscible oils as a filler material, which forms a barrier between the actuated droplets and the device surface (52, 53). This strategy has many other advantages and disadvantages (see Section 3.3). The second strategy is to control the solution pH and electrode polarity such that proteins are electrostatically repelled from surfaces (54). This strategy is effective for model systems containing one or a few analytes, but application to real samples is complicated by the presence of proteins with different charges and pIs. The third strategy is to use removable plastic films (55) in place of the more commonly used permanent dielectric layers described in Section 3.1. This approach is useful for preventing cross-contamination from experiment to experiment, but it does not suppress biofouling within a given experiment. The fourth strategy is to introduce nanostructures to render device surfaces superhydrophobic (56, 57). The self-cleaning effect of superhydrophobic surfaces diminishes the level of surface fouling; however, the fabrication process is complicated, and these surfaces are incompatible with surfactants. The fifth strategy is to add amphiphilic additives to liquids manipulated in DMF systems. Pluronics®, which are triblock copolymers of poly(ethylene oxide) and poly(propylene oxide), have been widely used as droplet additives to reduce biofouling in DMF systems (58, 59). This technique may not be universal, however, because reagents in some applications may not be compatible with Pluronics or other additives.

3.3. Integration with Other Techniques

A critical step in any microfluidic application is chemical analysis. DMF systems are commonly used for in-line analysis (in which constituents in droplets are analyzed within a device) and for off-line analysis (in which fractions are collected and analyzed outside of the device). Such usage stands in contrast to that of microchannel-based systems, which are well suited for in-line analysis but, in many cases, are not a perfect match for off-line analysis. In-line and off-line analysis systems for DMF (with a focus on combining DMF with detection and separations) are reviewed below.

Various techniques have been used to couple DMF to different types of detectors for in-line analysis. Srinivasan et al. (52, 60) reported a DMF system in which absorbance was measured in droplets with a light-emitting diode (LED) and a photodiode as a light source and a detector, respectively. Wijethunga et al. (61) used a light source and a camera for image-based absorbance monitoring of analyte concentration during liquid-liquid extraction in droplets. Compared with that of conventional spectrometers, the short optical path length of DMF systems is a limitation for methods relying on absorbance detection. In-line fluorescence detection in DMF systems has been demonstrated with a miniaturized fluorimeter consisting of an LED and a photodiode (30). In a similar approach, Lin et al. (62) integrated a semiconductor-based thin-film optical detector on a DMF device for chemiluminscence detection. Although strategies with integrated fluidics and detection (such as those described above) are useful for forming devices with a small footprint for eventual application in the field, modular approaches in which the detector is decoupled from the fluidics are particularly useful for laboratory instruments, and there have been numerous examples of coupling DMF with optical plate readers for absorbance (63) and fluorescence (55, 64–67) detection. Electrochemical detection has also been integrated with DMF chips for in-line analysis. Dubois et al. (68) integrated a catenary wire for electrochemical detection, and Poulos et al. (69) integrated thin-film Ag/AgCl electrodes. Other groups coupled electrochemical detectors with DMF by placing external electrodes on the tip of the device (46, 70). Malic et al. (71) coupled DMF with surface plasmon resonance imaging by using a gold layer deposited onto a top plate (**Figure 3*a***).

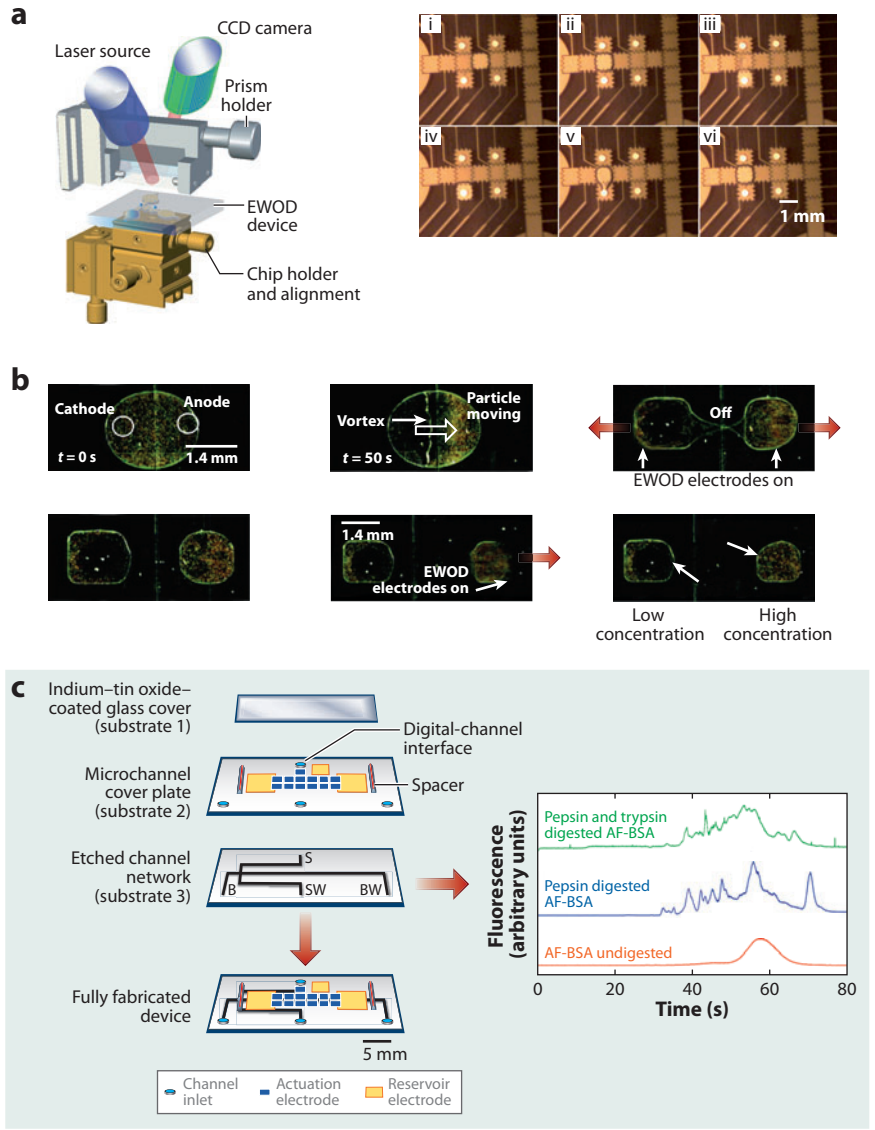

Figure 3

Coupling detectors and separations with digital microfluidics (DMF). (*a*) (*Left*) A DMF device coupled with surface plasmon resonance (SPR) detection. (*Right*) Video sequence depicting droplet movement over an array of SPR detection spots. Reproduced from Reference 71 with permission from the Royal Society of Chemistry. (*b*) Video sequence of particle concentration on DMF using electrophoresis. After the particles migrate toward the anode, the droplet is split. Reproduced from Reference 72 with permission from the Royal Society of Chemistry. (*c*) (*Left*) A multilayer hybrid device incorporating DMF on top and microchannels below. (*Right*) Electropherograms obtained after in-line enzymatic digestion of proteins in droplets. Reprinted with permission from Reference 78. Copyright 2010, American Chemical Society. Abbreviations: CCD, charge-coupled device; EWOD, electrowetting on dielectric; AF-BSA, Alexa Fluor 488–labeled bovine serum albumin.

Three techniques have been developed in DMF for in-line particle separation (in droplets), relying on electrophoresis, traveling-wave dielectrophoresis (twDEP), and optoelectronic tweezers (OET). In the first technique (**Figure 3*b***), Cho et al. (72) used electrophoresis to separate and concentrate particles. When dc potentials were applied to a droplet, the negatively and positively charged particles migrated to the anode and the cathode, respectively. After separation, the source droplet was split into two smaller droplets bearing the differently charged particles. To implement these separations, openings through the hydrophobic coating on the top plate were formed to allow for direct contact between the fluid and the electrodes. This method concentrated 83% of a given type of particle into daughter droplets. In the second technique, twDEP was coupled with DMF (73) to concentrate and separate noncharged particles. In this method, twDEP was used to transport particles within a droplet through the use of a specially designed twDEP electrode array. As above, after separation, the source droplet was split into daughter droplets. The system was configured with DEP electrodes on the bottom plate and DMF electrodes on the top plate; the DEP electrode array served as the ground electrode for DMF actuation. This system isolated 98% of the total particles into a daughter droplet. In the third technique, Shah et al. (74) combined OET with DMF. OET is a technique in which patterns of light are used to turn on so-called virtual electrodes to effect DEP. Through this technique, 68% of live cells (relative to dead cells) were concentrated into a daughter droplet.

Whereas the above examples describe in-line separations of particles, techniques have also been developed to separate molecular species on DMF devices through on-chip liquid-liquid extraction and solid-phase extraction techniques. Abdelgawad et al. (33) actuated aqueous droplets through water-immiscible solvent to remove the contaminants suppressing the ionization of DNA analytes in mass spectrometry (MS). Mousa et al. (75) drove the sample droplets into an isooctane pool to remove nonpolar constituents and enhance the purity of hormones in the samples. Wijethunga et al. (61) used ionic liquid droplet as extractant, decreasing the solvent consumption in liquid-liquid extraction. Yang et al. (76) performed solid-phase extraction by using porous polymer monolith (PPM) discs formed in situ. Peptide analytes were isolated from salt and surfactant through stepwise sample loading, rinsing, and elution from the PPM discs.

Although relatively simple separations on DMF devices have been demonstrated in line in droplets (as described above), more complex separations may require coupling with dedicated separation techniques. In such schemes, DMF is the sample-pretreatment system, and microchannels or column chromatography systems are used for separations. Abdelgawad et al. (77) coupled DMF with microchannel electrophoresis in a system in which a PDMS slab bearing a microchannel structure was bonded to a one-plate DMF device. DMF was used to label amino acids and cell lysate with a fluorescent derivatization agent, and the droplets were then injected into the PDMS microchannel for separations. Watson et al. (**Figure 3*c***) (78) improved upon this design by interfacing a two-plate DMF system on a top layer of a device with glass microchannels on a bottom layer through a vertical interconnect. The same strategy was used to couple DMF sample preparation to integrated microfluidic emitters for nanoelectrospray MS (79). In a related method, DMF was coupled with a portable capillary electrophoresis instrument (37). Sample droplets and run buffer droplets were actuated to the inlet of a separation capillary located on top of the electrode array. The analytes were concentrated through droplet evaporation in the single-plate format.

4. APPLICATIONS OF DIGITAL MICROFLUIDICS

Because DMF is a versatile fluid handling tool with many unique and useful features, it has been applied to a large number of applications in a wide range of fields. In the following subsections, we review these applications, which are categorized into six topics: chemical and enzymatic reactions

(Section 4.1), immunoassays (Section 4.2), DNA-based applications (Section 4.3), clinical diagnostics (Section 4.4), proteomics (Section 4.5), and cell-based applications (Section 4.6). Some applications straddle these classifications and are mentioned multiple times; for example, enzyme assays used for clinical diagnostic systems (80, 81) are described in both Sections 4.1 and 4.4. In selecting the examples described in the following sections, we omitted several unique applications of DMF that we deemed to be outside the broad rubric of analytical chemistry, including electronic cooling systems (82–87), particle sampling (57, 88, 89), microconveyor systems (90), and switchable dye lasers (91).

4.1. Chemical and Enzymatic Reactions

A fundamental application of DMF is the implementation of homogeneous chemical and enzymatic reactions. This application typically involves the precise metering of reactants by dispensing droplets from reservoirs and their subsequent merging and mixing to create isolated microreactors. Because each droplet can be controlled individually on a generic two-dimensional array of electrodes, many reactions can be carried out simultaneously on one device. As described above, oil-filled DMF systems have a number of advantages, but they are not suitable for some chemical synthesis applications that require organic solvents that are miscible with oil (92). In contrast, an open-air medium is useful in reactions that require solvent evaporation and is compatible with a wide range of liquids, including pure organic solvents and solutions, ionic liquids, and aqueous surfactant solutions (24).

Chemical and enzymatic reactions have been carried out in DMF to evaluate substances of interest, to study reaction kinetics, and to synthesize new compounds. In an early experiment, Taniguchi et al. (53) used a one-plate DMF device with a vegetable-oil filler medium to study two reactions. The first reaction was the alkalinization of phenolphthalein, which the authors performed by mixing droplets of NaOH and phenolphthalein to form a red-colored product. The second reaction was a luciferin-luciferase enzyme reaction, performed by mixing droplets of luciferin and ATP with luciferase to form a luminescent product. The same group (93) also carried out the first DMF-driven gas phase reaction by coalescing microsized reagent bubbles to induce an oxidation reaction.

Building on these early studies, other groups have developed assays for applications involving diagnostics and environmental detection. For example, Srinivasan et al. (60) optimized a colorimetric two-enzyme reaction in an oil-filled two-plate DMF device for the detection of glucose. The color change of the reaction was monitored with an integrated absorbance detector, which enabled the detection of glucose concentrations in the range from 25 to 300 mg dl^{-1}. To demonstrate the clinical applicability of this work, the same group (52) also performed the glucose assay on human physiological samples (whole blood, serum, urine, and saliva); the authors obtained values that mostly agreed with reference measurements. One exception was the case of the urine sample, in which the uric acid content significantly interfered with the enzymatic activity of the assay, exemplifying the importance of sample pretreatment for clinical diagnostics. The same group also developed chemical assays for environmental detection. For example, Pamula et al. (94) reported a DMF device for the detection of nitroaromatic explosives such as 2,4,6-trinitrotoluene (TNT). This colorimetric assay relies on the reaction between TNT and potassium hydroxide to form a colored Jackson-Meisenheimer complex. The authors demonstrated a linear range of detection for TNT between 4 μg ml^{-1} and 20 μg ml^{-1}; only 2.5 min were required for each reaction. For this experiment, the silicone oil carrier fluid was not compatible with common solvents for TNT analysis, such as acetone, acetonitrile, and methanol, so the authors were required to develop a modified assay with dimethyl sulfoxide (DMSO, which was immiscible with the carrier oil) as a

solvent (92). Similarly, the authors developed a chemical assay for the detection of sulfate particles from the environment. Because the traditional reagent solvent, ethanol, is miscible with silicone oil, alternative solvents were used for the assay. Recent research in enzyme assays has focused on improving analytical performance on DMF. For example, Vergauwe et al. (95) developed a software-based approach to select optimal actuation parameters (activation time, relaxation time, and voltage) to minimize the variability of droplet size during DMF manipulation. These parameters were validated by generation of a calibration curve for enzymatic glucose assays with an average CV of 2%.

In addition to quantifying substances of interest, DMF is particularly useful for studying enzyme kinetics and activity. For example, Miller & Wheeler (65) developed the first oil-free DMF device for enzyme assays and used it to study alkaline phosphatase (AP) kinetics and activity and to quantify fluorescein diphosphate (FDP) substrate. **Figure 4*a*** depicts an example of this assay, in which droplets of AP and FDP were merged and mixed to form fluorescein on a DMF device. The absence of oil makes this device compatible with a wider range of solvents and precludes the partitioning of hydrophobic analytes into the oil phase. Using this device, the authors evaluated the enzyme kinetics of AP and the effects of inhibition with inorganic phosphate, thereby producing kinetic constants that are consistent with those in the literature. In another example, Nichols & Gardeniers (96) designed a DMF method to investigate the pre–steady state kinetics of tyrosine phosphatase. This study was particularly challenging because the enzymatic reactions must be quenched in extremely short timescales (on the order of milliseconds). DMF facilitated these time-sensitive processes and the subsequent measurement by matrix-assisted laser desorption/ionization time-of-flight (MALDI-TOF)-MS, producing results that agree well with published data.

An emerging application of DMF is the chemical and enzymatic synthesis of new compounds. For example, Millman et al. (97) used a one-plate DMF device with an oil filler medium to synthesize microparticles with a range of characteristics, including polymer capsules, semiconducting microbeads, and anisotropic striped "eyeball" particles. In this format, droplets containing suspensions of micro- and nanoparticles, polymer solutions, and polymer precursors were merged, mixed, and dried to yield the different types of particles. This approach enabled the production of complex particles that are difficult to obtain with conventional synthetic techniques. In another example, Dubois et al. (68) performed Grieco's reaction by using ionic-liquid droplets as microreactors. Ionic liquids are advantageous because of their low vapor pressure—reactions can be implemented in relatively small (<1-μl) droplets on single-plate devices without the need for concern about evaporation. The authors performed in-line and off-line analysis of the final product, producing results that were comparable with those from a conventional reaction flask. In a

Figure 4

Chemical/enzyme reactions, immunoassays, and DNA-based applications implemented by digital microfluidics (DMF). (*a*) Video sequence of an enzymatic assay. Alkaline phosphatase (AP) and fluorescein diphosphate (FDP) were dispensed from their respective reservoirs, merged, and actively mixed to form fluorescein, a product that is visible under fluorescent illumination. Reprinted with permission from Reference 65. Copyright 2008, American Chemical Society. (*b*) Video sequence of five parallel chemical synthesis reactions. Droplets containing different amino acids (AA) were merged with aziridine aldehyde and *tert*-butyl isocyanide (tBuNC), and the reaction was allowed to proceed for 1 h. The cyclic peptide (CP) products were isolated by allowing the solvent to evaporate. Reprinted with permission from Reference 99. Copyright 2010, Wiley. (*c*) Protocol for heterogeneous magnetic bead–based immunoassay on a DMF platform. (*d*) Video sequence of magnetic bead washing performed by removing the excess supernatant on the chip. Reproduced from Reference 102 with permission from the Royal Society of Chemistry. (*e*) Four parallel DNA ligation reactions with insert vectors of various lengths. (*f*) Video sequence of a DNA ligation protocol. A droplet of vector DNA and insert DNA were merged and mixed; the pooled droplet was transported to the buffer solvent containing the DNA ligase enzyme to initiate the reaction. All droplets were surrounded by an oil shell to reduce the voltage required for droplet actuation. Reprinted from Reference 106 with permission. Copyright 2010, Elsevier.

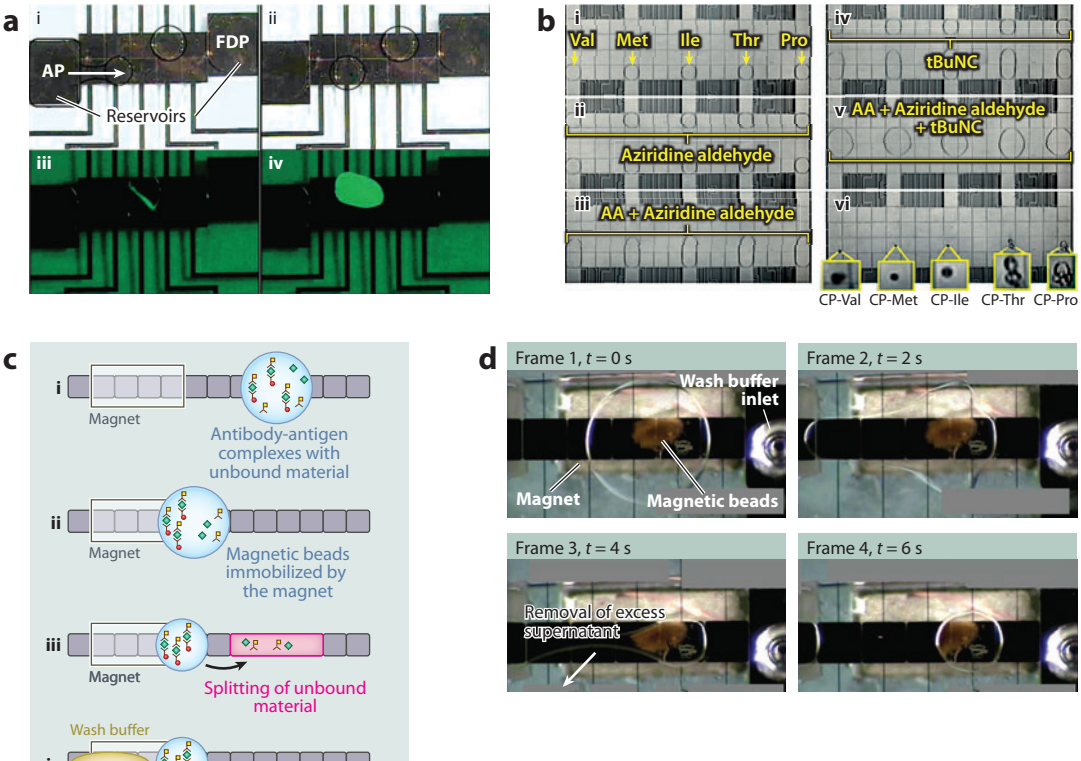

unique example, Martin et al. (98) created an artificial Golgi organelle by using DMF to mimic the enzymatic biosynthesis of heparin sulfate in vivo. In this experiment, immobilized heparin sulfate molecules on magnetic nanoparticles were modified by 3-*O*-sulfotransferase, which increased their affinity for fluorescently labeled antithrombin III as detected by confocal microscopy. The use of magnetic nanoparticles facilitated the removal of excess enzyme and reactants. This study demonstrated the feasibility of using DMF for the synthesis and screening of specific glycans.

Two recent examples in oil-free DMF devices relied on solvent evaporation and exchange to enable multistep chemical synthesis. In the first example, Jebrail et al. (99) demonstrated the synthesis of peptide macrocycles formed through the reaction of three components: amino acids, aziridine aldehyde, and *tert*-butyl isocyanide (tBuNC). The DMF device facilitated the implementation of synchronized synthesis of five different macrocycles in four steps (**Figure 4*b***). First, five 900-nl droplets containing one of five amino acid substrates (valine, methionine, isoleucine, threonine, and proline) were dispensed from their respective reservoirs. Second, five 900-nl droplets containing aziridine aldehyde were dispensed, merged with the amino acid droplets, and mixed. Third, five 900-nl droplets of tBuNC were dispensed, merged with the droplets containing the amino acids, and incubated. Finally, macrocyclic peptide products were isolated by allowing the solvent to evaporate. The authors demonstrated that the solid products can be further reacted in DMF to form aziridine ring–opened derivatives. The resulting products were identical to analogous products formed by macroscale methods, as shown by MS and NMR. In the second example, Keng et al. (100) demonstrated the synthesis of 2-[^{18}F]fluoro-2-deoxy-D-glucose ([^{18}F]-FDG), a common radio tracer used for imaging of living subjects with positron emission tomography (PET). The authors developed a DMF device with a dedicated reaction site capable of programmed Joule heating, droplet transport, and sensing/regulation of temperature. This design enabled rapid on-chip drying, solvent exchange, and reaction of fluorides, which facilitated the multistep synthesis of [^{18}F]-FDG. After on-chip synthesis, the products were purified off-chip, and the radio tracer was evaluated in in vivo biodistribution experiments by PET in lymphoma xenograft–bearing mice.

4.2. Immunoassays

An immunoassay is a technique that exploits specific antibody-antigen interactions for the detection of relevant analytes. In these assays, the primary task of antibodies is to bind to the analyte of interest, which can also be accomplished by other binding molecules, such as oligonucleic acids and peptide-based aptamers. To date, there have been at least five reports of immunoassays on DMF, all of which relied on antibodies immobilized on solid supports (i.e., heterogeneous immunoassays). In the earliest approach, Rastogi & Velev (101) developed immunoassays for immunoglobulin G (IgG) and ricin by relying on the agglutination patterns of antibody-coated latex and gold particles. A droplet suspended in fluorinated oil on a single-plate device served as a container with a controlled evaporation rate; the pattern assumed by the antibody-coated latex and the gold particles as the droplet evaporated indicated the quantity of antigen present in the sample. This method reduced sample volumes and limits of detection compared with commercially available methods, but produced a readout that may be difficult to standardize or automate for high-throughput analysis. In another example, Sista et al. (102) used an oil-filled DMF device to detect insulin and interleukin-6 by using droplets carrying paramagnetic beads modified with antibodies. As depicted in **Figure 4*c*,*d***, this immunoassay protocol was implemented in five steps:

1. A droplet containing magnetic beads, reporter antibodies, and blocking proteins (prepared off-chip) was merged and mixed with a droplet of analyte on-chip to form antibody-antigen complexes.

2. The reaction mixture was delivered to a permanent magnet to immobilize the magnetic beads.
3. The unbound supernatant was removed by splitting the excess liquid from the beads.
4. The unbound molecules were further washed by passing five droplets of wash buffer over the magnetic beads.
5. By use of the interfacial force of the droplet/oil interface, the magnetic beads were moved away from the magnet and resuspended for detection.

For detection, the enzymes on the reporter antibodies catalyzed a chemiluminescent signal that was detected by an integrated photomultiplier tube. To demonstrate the clinical applicability of this approach, the same group (30) performed troponin I immunoassays by using whole-blood samples; the authors obtained analyte recoveries ranging from 77% to 108%. In a recent experiment, Vergauwe et al. (103) explored the use of paramagnetic nanoparticles as a solid support for IgE immunoassays. The authors demonstrated that nanoparticles can be dispensed by DMF with reproducible densities (CV, 2.83%), which is critical for any analytical application. In these IgE immunoassays, a droplet containing magnetic nanoparticles (modified with anti-IgE) and fluorescently labeled IgE aptamer was merged and mixed with a second droplet containing a nonlabeled IgE sample. Magnetic bead washing was performed in a similar manner as that described above. The assay was capable of detecting IgE at concentrations as low as 150 nM.

An alternative to the use of beads as solid support for heterogeneous immunoassays is the direct immobilization of capture antibodies on the device surface. Miller et al. (67) demonstrated the first surface-based immunoassay on DMF by using human IgG as a model analyte. In this study, capture antibodies were physisorbed on the hydrophobic surface of a DMF device. The bound analyte was detected through the use of FITC (fluorescein isothiocyanate)-labeled anti-IgG, and after the final wash, the fluorescence was measured in a fluorescence plate reader. To aid in droplet movement and prevent nonspecific adsorption (see Section 3.2), the authors used Pluronics F-127 as an additive to the assay solutions, which eliminated the need for an oil carrier fluid. The absence of an oil barrier surrounding the droplet was critical for this assay because oil probably would interfere with antibody-antigen binding events occurring at the surface.

4.3. DNA-Based Applications

The manipulation and characterization of DNA samples are critical processes in numerous fields, such as pharmaceutical research, medical diagnostics, gene therapy, and forensics. These processes tend to be performed on small, precious samples and/or in a highly multiplexed format, making them a natural fit for microfluidics. Thus, there is a great deal of interest in the use of DMF to develop fluidic microprocessors and small-volume microreactors for DNA-based applications. In particular, DMF has been employed for the purification and extraction of DNA samples, generating recombinant DNA by ligation, DNA hybridization assays, polymerase chain reaction (PCR), and pyrosequencing.

Before DNA samples are analyzed or characterized, they must be purified and extracted from complex mixtures. For example, Abdelgawad et al. (33) purified a DNA sample from a complex mixture by using DMF to implement liquid-liquid extraction. In this experiment, aqueous droplets containing a mixture of DNA and proteins were driven into and out of a pool of phenolic oil, which removed proteins from the droplet and purified the nucleic acid. In another example, Sista et al. (30) extracted human genomic DNA from a whole-blood sample on an oil-filled two-plate DMF device. In this study, droplets of whole blood were merged and mixed with lysis buffer. The resulting droplets of cell lysate were then combined with paramagnetic DNA capture beads in succession. At the same time, with the help of a magnet, the authors removed the unbound

supernatant by splitting the excess liquid from the beads. The DNA was purified by passing droplets of wash buffer over the beads, removing the remaining cell debris. Finally, the DNA captured on the beads was eluted, which enabled collection and subsequent processing on- or off-chip. A similar process was employed to isolate *Mycoplasma pneumoniae*–specific DNA from patient samples by use of an appropriate biotinylated capture probe and streptavidin-coupled magnetic beads (104).

DMF devices have also been used as microfluidic reactors for DNA ligation to generate recombinant DNA for cloning applications. In the first demonstration of this technique, Liu et al. (105) developed an oil-free DMF device that facilitated DNA ligation by merging droplets containing vector DNA and insert DNA into a buffer reservoir containing DNA ligase. This approach had a total reaction volume of 2.1 μl, whereas a comparable macroscale method consumes 15 μl of reagent (of which only 2 μl is required to transform cells). This substantial reduction in reagent waste makes this DMF device an economical tool for molecular cloning. In an improvement on this work, the same group (106) implemented three design changes: (*a*) adoption of a water-oil core-shell approach and a thinner insulator to reduce voltage requirement of droplet actuation, (*b*) optimization of the droplet-mixing sequence and incubation time to improve the efficiency of DNA ligation, and (*c*) development of a design to facilitate four parallel DNA ligation reactions. **Figure 4*e*** illustrates this design scheme and the DNA ligation protocol. As shown, four droplets of insert DNA of various lengths were dispensed on the left from their respective reservoirs and merged with the vector droplets in the center. The pooled droplets were transported and merged with the reservoirs containing DNA ligase (**Figure 4*f***). After the DNA ligase reaction, the resulting recombinant DNA was taken off-chip and transformed into bacteria. The transformed bacteria were cultured overnight, and white colony plasmids were extracted and analyzed by electrophoresis to confirm the presence of the insert DNA fragment. In the future, the authors propose to integrate these off-chip functions by using DMF to realize an efficient DNA cloning system for synthetic biology applications.

Hybridization is a unique process in which single strands of nucleic acids interact with their complementary strands; this phenomenon is often exploited for the detection of specific DNA sequences. DMF devices are well suited for hybridization assays. For example, Malic et al. (107) developed a unique DMF two-plate platform coupled to surface plasmon resonance imaging (SPRi) for multiplexed, real-time, label-free detection of DNA hybridization on the device surface. The device's top plate was modified to expose bare gold spots that were surrounded by hydrophobic Teflon AF for the immobilization of DNA probes. Interestingly, the DMF architecture imbued this platform with two unique advantages: (*a*) Distinct DNA probes can be simultaneously immobilized at designated detection sites, and (*b*) the voltage applied to the electrodes can enhance hybridization efficiency by twofold. Building on this experiment, the same authors (108) fabricated gold nanoposts at the detection sites to enhance the SPRi signal by 200%, achieving a limit of detection of 500 pM. In the future, the authors propose to integrate more detection sites to increase the throughput of hybridization assays.

One of the most powerful DNA-based techniques is PCR, which is used to amplify small amounts of DNA to generate millions of copies of a specific sequence. An essential component of PCR is the thermal cycling between low (60°C) and high (95°C) temperatures to carry out each step within the amplification cycle. Conveniently, DMF is well suited for precise on-chip temperature control of reagent droplets because the large surface area–to–volume ratio of the droplets enables efficient heat transfer. Thus, it is not surprising that implementation of PCR on DMF has attracted a great deal of attention in the field. In an early example, Chang et al. (109) developed a DMF device with an embedded microheater to facilitate thermal cycling. In this study, droplets containing an oligonucleotide to be amplified and PCR reagents were merged, mixed,

and then delivered to the integrated heater. The fluorescent signals from DNA amplified on-chip were comparable to those generated from a bench-scale PCR machine; the total time and sample consumption were reduced by 50% and 70%, respectively. Improving on this technique, Sista et al. (30) developed a DMF device with two different temperature zones and performed PCR by shuttling the amplification droplet between these zones. This design facilitated the completion of a 40-cycle real-time PCR within 12 min. More recently, the same group (110) expanded on this design to develop an automated and self-contained multichannel DMF platform for multiplexed real-time PCR. The entire system is the size of a shoebox and contains all of the required control and detection capabilities, along with a disposable microfluidic cartridge in which sample processing and PCR take place (**Figure 5*a***). To facilitate parallel-scale sample preparation and PCR, the system has four cylindrical neodymium magnets for paramagnetic bead manipulation and four miniature fluorimeter modules consisting of four independent and spatially separated channels. To investigate the sensitivity of the system, the authors performed a titration experiment by using 10-fold dilutions of DNA samples ranging from 307 pg to 3.07 fg of DNA input. The system has an amplification efficiency of 94.7% and can detect the equivalent of a single genome of test samples (methicillin-resistant *Staphylococcus aureus*). As a proof of concept for high-throughput multiplexed PCR applications, the authors demonstrated that multiple DNA samples can be amplified and detected simultaneously.

An emerging DNA-based application in DMF is pyrosequencing, in which DNA is sequenced by synthesizing its complement through a series of enzymatic reactions with a chemiluminescent reporter. Recently, Welch et al. (111) tested the feasibility of implementing pyrosequencing by using DMF. Because DNA is immobilized on magnetic beads for this application, the authors developed techniques to improve the reproducibility of magnetic bead dispensing by strategically positioning magnets near the reservoir. They also demonstrated that ATP can be detected at 7 nM, which is below the expected concentration arising from a single-nucleotide addition.

4.4. Clinical Diagnostics

Clinical diagnostics can be divided into four sequential stages: sample collection, sample preparation, analytical processing, and detection (4). DMF has been used primarily to address problems in stages 2 and 3 (sample preparation and analytical processing). In one example, Wulff-Burchfield et al. (104) performed DMF-based PCR to detect *Mycoplasma pneumoniae* DNA in respiratory specimens obtained from patients with community-acquired pneumonia. The authors employed the multiplexed DMF platform described above (**Figure 5*a***) to carry out real-time PCR and observed 98% agreement between the DMF approach and a reference method for detection of *Mycoplasma* DNA. Although sample preparation was performed manually for both methods, the DMF approach incorporated a magnetic bead concentration step to compensate for the smaller reaction volume. Compared with the reference method, the DMF approach was three times faster and maintained a similar analytical performance. Using a related DMF platform, Sista et al. (80, 81) carried out multiplexed enzymatic analysis to screen for lysosomal storage diseases (LSDs) in newborn patient samples. For this application, sample preparation was performed manually in well plates to extract patient samples from dried blood spot (DBS) samples stored on filter paper punches (3.2 mm in diameter). In the first study (81), the authors screened for Hunter syndrome, which is caused by deficiency in iduronate-2-sulfatase (IDS), by using a two-step enzymatic assay to form a fluorescent product. With this scheme, the authors measured the IDS activity in DBS from 106 normal newborn specimens and 6 Hunter syndrome patients. The DMF enzymatic assay discriminated between the 6 Hunter syndrome patients and the 106 normal newborns (**Figure 5*b***). Remarkably, the authors observed a drastic reduction in analysis time (28 h to 1 h)

and in reagent consumption (10 µl to 300 nl). In the second study (80), the authors demonstrated similar success for two other LSDs (Pompe and Fabry disorders).

Jebrail et al. (79) recently demonstrated a DMF method for the extraction and analysis of amino acids for use in diagnosing genetic disorders directly from DBS samples taken from newborn patients. In this study, analytes were extracted from the DBS, mixed with internal standards, derivatized, and reconstituted for analysis by (off-line and in-line) tandem MS (**Figure 5*c***). Using

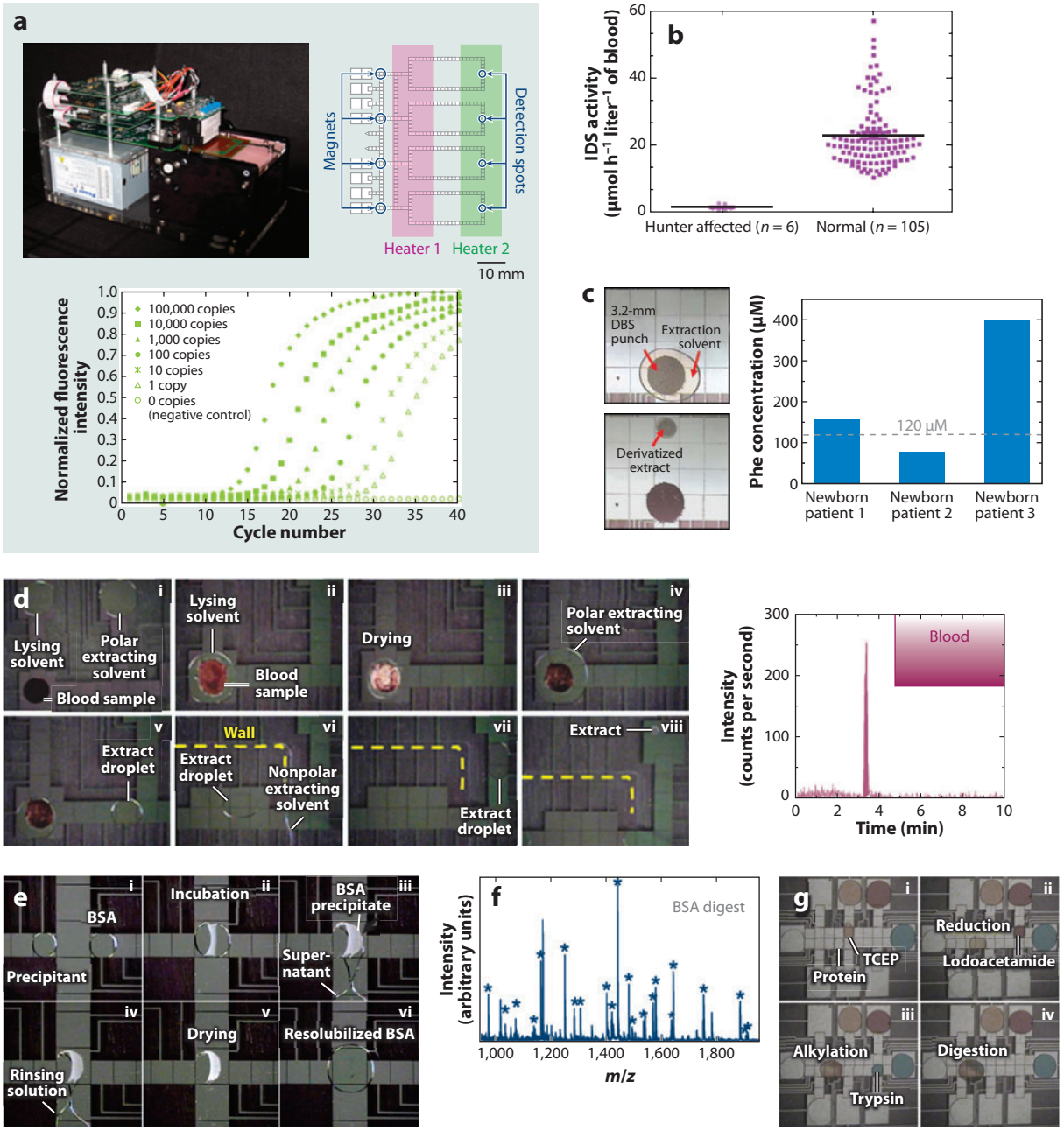

this approach, the authors evaluated DBS punches from three newborn patients to screen them for phenylketonuria. This technique correctly identified patients 1 and 3 as diseased and patient 2 as unaffected (**Figure 5*c***). In another example, a DMF-driven method was reported for sample cleanup and extraction of estradiol in 1-μl samples of human breast tissue homogenate, as well as from whole blood and serum (75). In a typical assay, the sample was chemically lysed, the estradiol was extracted into a polar solvent, unwanted constituents were extracted into a nonpolar solvent, and the extract was delivered to a collection reservoir for off-chip analysis (**Figure 5*d***). Extracted estradiol from 1-μl samples (e.g., breast tissue homogenate from a postmenopausal breast cancer patient) was detected with a high signal-to-noise ratio with liquid chromatography tandem MS with selected reaction monitoring and quantified with enzyme-linked immunosorbent assay. The DMF method employed a sample size that was 1,000-fold smaller than the conventional methods for extraction and quantification of steroids and was 20 times faster. The small sample requirement could enable the routine screening of breast tissue samples for the diagnosis and prognosis of breast cancer.

4.5. Proteomics

Proteomic experiments typically require tedious, multistep sample processing before analysis by mass spectrometers or other detectors can be performed, and the ability of DMF to individually address many reagents simultaneously makes it a good fit for such processes. In an early demonstration of proteomics in a DMF format, DMF-based methods were developed to purify peptides and proteins from heterogeneous mixtures (112, 113). These methods comprised a series of steps, including drying the sample droplet, rinsing the dried spot with deionized water droplets to remove impurities, and finally delivering a droplet of MALDI matrix to the purified proteins for on-chip analysis by MS. The authors of these studies then improved this process by implementing simultaneous purification of six samples (114). Recently, a DMF-based protocol was developed for extracting and purifying proteins from complex biological mixtures by precipitation, rinsing, and resolubilization (**Figure 5*e***) (115). The method had protein recovery efficiencies (~80%)

Figure 5

Clinical diagnostics and proteomics in digital microfluidics (DMF). (*a*) (*Top left*) A self-contained DMF system for multiplexed real-time polymerase chain reaction (PCR). (*Top right*) A printed circuit board schematic for PCR, showing electrode positions relative to heaters, magnets, and detectors. (*Bottom*) Representative real-time PCR data of bacterial genomic DNA prepared by DMF-driven processing. Reprinted with permission from Reference 110. Copyright 2010, American Chemical Society. (*b*) Iduronate-2-sulfatase (IDS) activity measured in dried blood spot (DBS) extracts from Hunter syndrome patients and random newborn screening specimens. Reprinted with permission from Reference 81. Copyright 2011, Elsevier. (*c*) (*Left*) Video sequence depicting sample processing of a 3.2-mm-diameter punch from a DBS on filter paper. (*Right*) Graph of phenylalanine (Phe) concentrations from patient samples, processed by DMF. The dashed line indicates the upper level for normal concentrations of Phe in newborn blood samples; patients 1 and 3 were correctly identified as suffering from phenylketonuria. Reproduced from Reference 79 with permission from the Royal Society of Chemistry. (*d*) (*Left*) Video sequence illustrating key steps in DMF-based extraction of estrogen from 1 μl of human blood. (*Right*) Representative chromatogram of estradiol extracted from a human blood sample, generated by liquid chromatography tandem mass spectrometry with selected reaction monitoring. Reprinted from Reference 75 with permission from AAAS. (*e*) Video sequence depicting the extraction and purification of proteins by precipitation. A droplet of bovine serum albumin (BSA) was merged with precipitant to form the protein precipitant on the device's surface. The precipitant was washed with rinsing solution and resolubilized in a droplet of borate buffer for subsequent processing. Reprinted with permission from Reference 115. Copyright 2008, American Chemical Society. (*f*) A representative MALDI-MS (matrix-assisted laser desorption/ionization mass spectrometry) spectrum of BSA prepared by DMF-driven processing. Reprinted with permission from Reference 66. Copyright 2008, American Chemical Society. (*g*) Frames from a video illustrating sequential reduction, alkylation, and digestion of a droplet of resolubilized protein. Abbreviation: TCEP, *tris*(2-carboxyethyl)phosphine. Reproduced with permission from Reference 120. Copyright 2009, JoVE.

comparable to those of conventional techniques, and they required no centrifugation and less processing time. In a separate study, DMF was applied to key proteomic processing steps that commonly follow protein extraction, including protein reduction, alkylation, and digestion (66). Peptide mixtures processed in this manner were analyzed off-chip by MALDI-MS and were identified by a Mascot database search engine, which yielded correct sample identification with a confidence level greater than 95% (**Figure 5*f***). In related research, on-chip protein biochemical processing was combined with in situ analysis by MALDI-MS (116). The authors of that study also integrated a heater on DMF to increase sample-processing efficiency (117). In an alternative strategy, DMF has recently been used to deliver reagents to and from hydrogel discs (118), and this system has proven to be particularly powerful for forming heterogeneous microreactors for proteomic sample digestion (119) that are more efficient and have higher sequence coverage relative to homogeneous digestions (as described above). For a complete proteomic sample workup, an automated DMF-based platform was developed; this platform integrated all the commonly used processes, including protein precipitation, rinsing, resolubilization, reduction, alkylation, and digestion (**Figure 5*g***) (120). Finally, as described in Section 3.2, DMF was integrated with microchannels for in-line sample processing and separation, which has been useful for proteomic analysis (77, 78).

4.6. Cell-Based Applications

Cell-based applications have been a popular target for miniaturization because the required reagents and other materials are often prohibitively expensive. However, these applications can be challenging to implement on DMF because cells must be transported without alteration to their function or viability. Therefore, oil-filled DMF devices are probably incompatible with this application, given that silicone oil may restrict the exchange of gases between cells and the atmosphere (121). In addition, cells and proteins are likely to adsorb onto hydrophobic surfaces, which would render the droplets immovable on the DMF device. Despite these challenges, there has been a recent surge of publications in this area that have demonstrated new DMF methods for cell-based assays, cell sorting, and cell culture.

Barbulovic-Nad et al. (64) reported the first cell-based assay implemented by DMF. In this study, a Pluronics additive enabled the actuation of cell suspensions with densities as high as 6×10^7 cells ml^{-1} (**Figure 6*a***). The authors reported a toxicology-screening assay in which droplets carrying Jurkat T cells were merged with droplets containing different concentrations of the surfactant Tween® 20 (lethal to cells) and were then merged again with droplets carrying viability dyes (**Figure 6*a***). The DMF assay was more sensitive than an identical one performed in a 384-well plate, such that the DMF-generated results gave a better approximation of the empirical value of the 100% lethal concentration and also demonstrated a 30-fold reduction in reagent consumption. Additionally, actuation by DMF had no significant effects on cell vitality. In a more recent example, Park et al. (122) exploited the versatility of DMF to characterize various cryoprotective agent mixtures. These authors used DMF to prepare droplets containing various ratios of DMSO-PBS mixtures with or without cells. After the droplets were subjected to freezing and thawing, they were further mixed with viability dyes to assess their postthaw viability. Finally, Fiddes et al. (118) recently reported a DMF system to deliver media and other reagents to three-dimensional networks of cells growing in hydrogel discs, a format that will probably be useful for tissue engineers interested in screening conditions for forming three-dimensional scaffolds of cells.

Three techniques have been implemented in DMF to sort and manipulate cells inside droplets by use of electrical, optical, or magnetic forces. In the first technique, Fan et al. (123) used

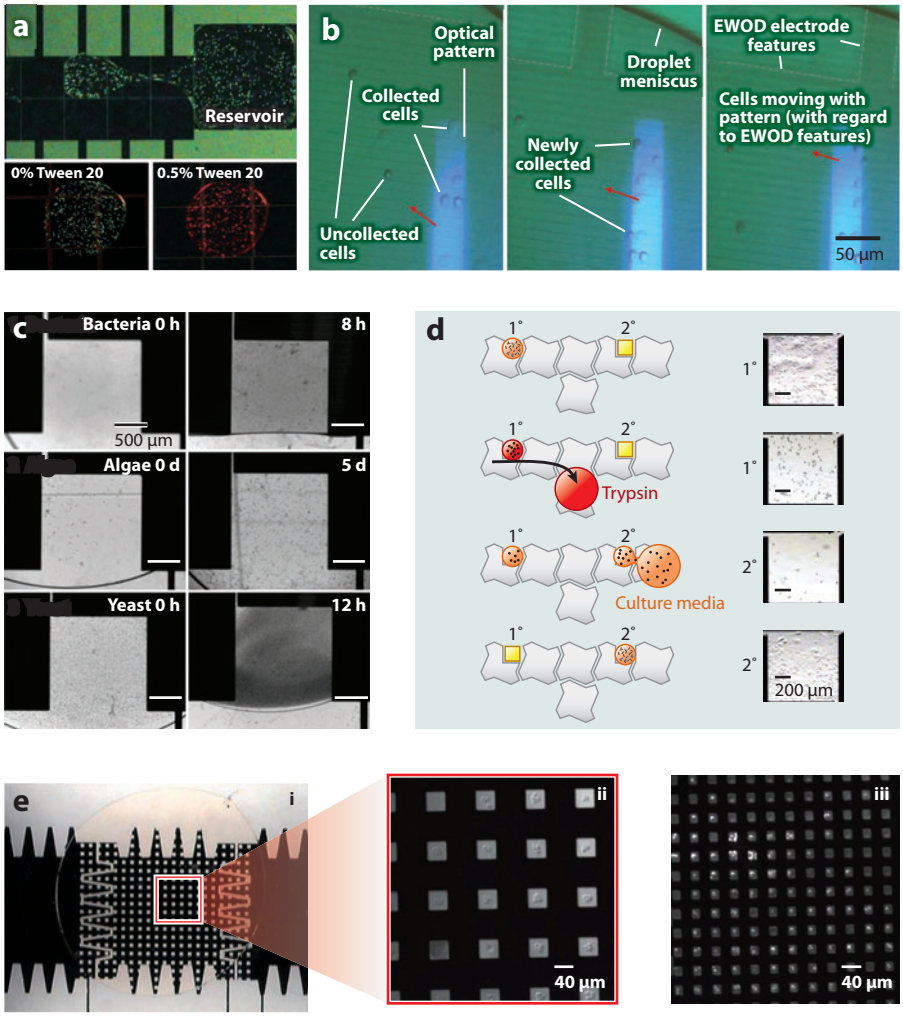

Figure 6

Cell-based applications in digital microfluidics (DMF). (*a*) Cell-based toxicity assays by DMF. (*Top*) A droplet carrying Jurkat T cells labeled with calcein AM (which fluoresces green) that are being dispensed from a reservoir. (*Bottom*) Droplets containing cells challenged with (*left*) 0% and (*right*) 0.5% Tween® 20. Cells exposed to high concentrations of Tween 20 undergo necrosis and fluoresce red when labeled with ethidium homodimer 1. Reproduced from Reference 64 with permission from the Royal Society of Chemistry. (*b*) Video sequence depicting cell manipulation and collection on a DMF device by lateral field optoelectronic tweezers. Red arrows indicate the movement direction of optical pattern. Abbreviation: EWOD, electrowetting on dielectric. Reproduced from Reference 74 with permission from the Royal Society of Chemistry. (*c*) Droplets containing microorganisms (bacteria, algae, and yeast) positioned on an L-shaped DMF electrode for absorbance detection at various culture times. Reproduced from Reference 63 with permission from Springer. (*d*) (*Left*) Schematic and (*right*) pictures depicting a subculture of CHO-K1 cells in droplets by DMF. Reproduced from Reference 125 with permission from the Royal Society of Chemistry. (*e*) (*i*) A droplet of HeLa cells incubated on a DMF electrode modified with an array of poly-L-lysine (PLL) micropatches to promote cell adhesion. (*ii*) Clusters of HeLa cells on 40 μm × 40 μm PLL patches. (*iii*) Single HeLa cells on 15 μm × 15 μm PLL patches. Reproduced from Reference 129 with permission from the Royal Society of Chemistry.

dielectrophoresis to separate neuroblastoma cells to different regions of droplets in a DMF device. The original droplets were then split into daughter droplets containing different cell densities. In the second technique, Shah et al. (74) developed an integrated DMF-lateral field OET microfluidic device for cell handling, in which the cells were attracted to the optical pattern illuminated on the DMF device (**Figure 6*b***). When this optical pattern moved to the left, more cells were collected and the collected cells continued moving with the pattern. In the third technique, the same group (124) exploited magnetic forces to concentrate specific cell populations in DMF. In this study, a droplet containing antibody-conjugated magnetic beads was merged with a droplet containing a mixture of $CD8^+$ and $CD8^-$ T lymphocyte cells. In the pooled droplet, the $CD8^+$ cells selectively bound to the magnetic beads, and an external magnet was used to purify these cells.

Techniques for cell culture on DMF are being developed that are compatible with both suspension cells and adherent cells. In an example of suspension culture, a platform was developed to culture bacteria, algae and yeast (63). These microorganisms were grown on-chip for up to five days with an automated semicontinuous mixing and temperature control. The cell densities were determined by measurement of absorbances through transparent regions of the devices (**Figure 6*c***). Growth profiles generated in the DMF device were comparable to those generated in macroscale systems. In an example of a system suitable for adherent cells, Barbulovic-Nad et al. (125) developed the first microfluidic platform capable of implementing all of the steps required for mammalian adherent cell culture–cell seeding, growth, detachment, and reseeding on a fresh surface (**Figure 6*d***). Three key innovations enabled the implementation of complete mammalian cell culture (i.e., with passaging for growth of multiple generations) on a microfluidic device: (*a*) a technique for growing cells on patterned islands (or adhesion pads) positioned on an array of DMF actuation electrodes, (*b*) a method for rapidly and efficiently exchanging media and other reagents on cells grown on adhesion pads, and (*c*) a system capable of detachment and collection of cells from an (old) origin site and delivery to a (new) destination site for subculture. Innovation *b* allows for high-precision metering of reagents to cells grown in self-contained droplets known as virtual microwells (126) and has recently proven useful for the culture and analysis of primary cells (127) and for multiplexed apoptosis assays (128). Building on these methods, Lammertyn and coworkers (103, 129) developed a technique to form micrometer-dimension adhesion pads for adherent cell culture and assay. Such precise fabrication allowed the cells to be arrayed as cell clusters (40-μm pads) or as single cells (15-μm pads) (**Figure 6*e***).

5. CONCLUSIONS AND FUTURE OUTLOOK

In this review, we summarize the state of the art in DMF technology in sections describing the theory of droplet actuation, device fabrication and integration, and applications. With the advent of PCB-based devices, removable film technology, and rapid prototyping techniques, DMF is becoming cheaper and more accessible in both industry and research settings. The capabilities of DMF continue to improve as novel techniques for droplet actuation, detection, and separation are adapted to this format. For example, the emerging electrode-less actuation techniques relying on optical forces, magnetism, thermocapillary forces, and SAWs are still new, and as they improve, they will make DMF devices even more versatile and compact. DMF has demonstrated advantages in applications in many different fields, especially in proteomics and clinical diagnostics, in which complex samples can be pretreated and analyzed on a single device. Furthermore, we propose that DMF technology will be promising for point-of-care and field tests, given that rugged and compact instruments with no moving parts can be produced and require no special skill to operate.

At present, however, the use of DMF technology is limited, mainly due to the complicated fabrication process of DMF devices (compared with, for example, soft lithography for microchannels) and the lack of commercial instrumentation. We anticipate that this situation will change with the development of mass production techniques and general-purpose DMF instruments. In summary, although DMF technology is still immature, it is continuously improving and has great potential to contribute significantly to applications in analytical chemistry and beyond.

DISCLOSURE STATEMENT

The authors are not aware of any affiliations, memberships, funding, or financial holdings that might be perceived as affecting the objectivity of this review.

ACKNOWLEDGMENTS

We thank the Natural Sciences and Engineering Research Council of Canada (NSERC) for financial support. A.H.C.N. and R.F. thank NSERC for graduate fellowships, and A.R.W. thanks the Canada Research Chair (CRC) Program for a CRC.

LITERATURE CITED

1. Abdelgawad M, Wheeler AR. 2009. The digital revolution: a new paradigm for microfluidics. *Adv. Mater.* 21:920–25
2. Miller EM, Wheeler AR. 2009. Digital bioanalysis. *Anal. Bioanal. Chem.* 393:419–26
3. Jebrail MJ, Wheeler AR. 2010. Let's get digital: digitizing chemical biology with microfluidics. *Curr. Opin. Chem. Biol.* 14:574–81
4. Pollack MG, Pamula VK, Srinivasan V, Eckhardt AE. 2011. Applications of electrowetting-based digital microfluidics in clinical diagnostics. *Expert Rev. Mol. Diagn.* 11:393–407
5. Cho SK, Moon H. 2008. Electrowetting on dielectric (EWOD): new tool for bio/micro fluids handling. *BioChip J.* 2:79–96
6. Malic L, Brassard D, Veres T, Tabrizian M. 2010. Integration and detection of biochemical assays in digital microfluidic LOC devices. *Lab Chip* 10:418–31
7. Wheeler AR. 2008. Putting electrowetting to work. *Science* 322:539–40
8. Huebner A, Sharma S, Srisa-Art M, Hollfelder F, Edel JB, de Mello AJ. 2008. Microdroplets: a sea of applications? *Lab Chip* 8:1244–54
9. Theberge AB, Courtois F, Schaerli Y, Fischlechner M, Abell C, et al. 2010. Microdroplets in microfluidics: an evolving platform for discoveries in chemistry and biology. *Angew. Chem. Int. Ed.* 49:5846–68
10. Pompano RR, Liu W, Du W, Ismagilov RF. 2011. Microfluidics using spatially defined arrays of droplets in one, two, and three dimensions. *Annu. Rev. Anal. Chem.* 4:59–81
11. Washizu M. 1998. Electrostatic actuation of liquid droplets for microreactor applications. *IEEE Trans. Ind. Appl.* 34:732–37
12. Pollack MG, Fair RB, Shenderov AD. 2000. Electrowetting-based actuation of liquid droplets for microfluidic applications. *Appl. Phys. Lett.* 77:1725–26
13. Pollack MG, Shenderov AD, Fair RB. 2002. Electrowetting-based actuation of droplets for integrated microfluidics. *Lab Chip* 2:96–101
14. Cho SK, Moon H, Kim CJ. 2003. Creating, transporting, cutting, and merging liquid droplets by electrowetting-based actuation for digital microfluidic circuits. *J. Microelectromech. Syst.* 12:70–80
15. Berthier J, Dubois P, Clementz P, Claustre P, Peponnet C, Fouillet Y. 2007. Actuation potentials and capillary forces in electrowetting based microsystems. *Sens. Actuators A Phys.* 134:471–79
16. Quilliet C, Berge B. 2001. Electrowetting: a recent outbreak. *Curr. Opin. Colloid Interface Sci.* 6:34–39
17. Berge B. 1993. Electrocapillarity and wetting of insulator films by water. *C. R. Acad. Sci. II* 317:157–63
18. Jones TB. 2002. On the relationship of dielectrophoresis and electrowetting. *Langmuir* 18:4437–43

19. Jones TB, Fowler JD, Chang YS, Kim CJ. 2003. Frequency-based relationship of electrowetting and dielectrophoretic liquid microactuation. *Langmuir* 19:7646–51
20. Jones TB, Wang KL, Yao DJ. 2004. Frequency-dependent electromechanics of aqueous liquids: electrowetting and dielectrophoresis. *Langmuir* 20:2813–18
21. Chatterjee D, Shepherd H, Garrell RL. 2009. Electromechanical model for actuating liquids in a two-plate droplet microfluidic device. *Lab Chip* 9:1219–29
22. Zeng J, Korsmeyer T. 2004. Principles of droplet electrohydrodynamics for lab-on-a-chip. *Lab Chip* 4:265–77
23. Wang W, Jones TB. 2011. Microfluidic actuation of insulating liquid droplets in a parallel-plate device. *J. Phys. Conf. Ser.* 301:012057
24. Chatterjee D, Hetayothin B, Wheeler AR, King DJ, Garrell RL. 2006. Droplet-based microfluidics with nonaqueous solvents and solutions. *Lab Chip* 6:199–206
25. Song JH, Evans R, Lin YY, Hsu BN, Fair RB. 2008. A scaling model for electrowetting-on-dielectric microfluidic actuators. *Microfluid. Nanofluid.* 7:75–89
26. Peykov V, Quinn A, Ralston J. 2000. Electrowetting: a model for contact-angle saturation. *Colloid Polym. Sci.* 278:789–93
27. Vallet M, Vallade M, Berge B. 1999. Limiting phenomena for the spreading of water on polymer films by electrowetting. *Eur. Phys. J. B* 11:583–91
28. Verheijen HJJ, Prins MWJ. 1999. Reversible electrowetting and trapping of charge: model and experiments. *Langmuir* 15:6616–20
29. Mugele F, Herminghaus S. 2002. Electrostatic stabilization of fluid microstructures. *Appl. Phys. Lett.* 81:2303–5
30. Sista R, Hua Z, Thwar P, Sudarsan A, Srinivasan V, et al. 2008. Development of a digital microfluidic platform for point of care testing. *Lab Chip* 8:2091–104
31. Gong J, Kim CJ. 2008. All-electronic droplet generation on-chip with real-time feedback control for EWOD digital microfluidics. *Lab Chip* 8:898–906
32. Gong J, Kim CJ. 2008. Direct-referencing two-dimensional-array digital microfluidics using multilayer printed circuit board. *J. Microelectromech. Syst.* 17:257–64
33. Abdelgawad M, Freire SL, Yang H, Wheeler AR. 2008. All-terrain droplet actuation. *Lab Chip* 8:672–77
34. Watson MWL, Abdelgawad M, Ye G, Yonson N, Trottier J, Wheeler AR. 2006. Microcontact printing-based fabrication of digital microfluidic devices. *Anal. Chem.* 78:7877–85
35. Abdelgawad M, Wheeler AR. 2007. Rapid prototyping in copper substrates for digital microfluidics. *Adv. Mater.* 19:133–37
36. Abdelgawad M, Wheeler AR. 2008. Low-cost, rapid-prototyping of digital microfluidics devices. *Microfluid. Nanofluid.* 4:349–55
37. Gorbatsova J, Jaanus M, Kaljurand M. 2009. Digital microfluidic sampler for a portable capillary electropherograph. *Anal. Chem.* 81:8590–95
38. Brassard D, Malic L, Normandin F, Tabrizian M, Veres T. 2008. Water-oil core-shell droplets for electrowetting-based digital microfluidic devices. *Lab Chip* 8:1342–49
39. Fan SK, Hsu YW, Chen CH. 2011. Encapsulated droplets with metered and removable oil shells by electrowetting and dielectrophoresis. *Lab Chip* 11:2500–8
40. Chiou PY, Moon H, Toshiyoshi H, Kim CJ, Wu MC. 2003. Light actuation of liquid by optoelectrowetting. *Sens. Actuators A Phys.* 104:222–28
41. Chuang HS, Kumar A, Wereley ST. 2008. Open optoelectrowetting droplet actuation. *Appl. Phys. Lett.* 93:064104
42. Chiou PY, Park SY, Wu MC. 2008. Continuous optoelectrowetting for picoliter droplet manipulation. *Appl. Phys. Lett.* 93:221110
43. Chiou PY, Chang Z, Wu MC. 2008. Droplet manipulation with light on optoelectrowetting device. *J. Microelectromech. Syst.* 17:133–38
44. Park SY, Teitell MA, Chiou EPY. 2010. Single-sided continuous optoelectrowetting (SCOEW) for droplet manipulation with light patterns. *Lab Chip* 10:1655–61
45. Guo ZG, Zhou F, Hao JC, Liang YM, Liu WM, Huck WTS. 2006. "Stick and slide" ferrofluidic droplets on superhydrophobic surfaces. *Appl. Phys. Lett.* 89:081911

46. Garcia AA, Egatz-Gomez A, Lindsay SA, Dominguez-Garcia P, Melle S, et al. 2007. Magnetic movement of biological fluid droplets. *J. Magn. Magn. Mater.* 311:238–43
47. Darhuber AA, Valentino JP, Troian SM, Wagner S. 2003. Thermocapillary actuation of droplets on chemically patterned surfaces by programmable microheater arrays. *J. Microelectromech. Syst.* 12:873–79
48. Darhuber AA, Valentino JP, Troian SM. 2010. Planar digital nanoliter dispensing system based on thermocapillary actuation. *Lab Chip* 10:1061–71
49. Guttenberg Z, Muller H, Habermuller H, Geisbauer A, Pipper J, et al. 2005. Planar chip device for PCR and hybridization with surface acoustic wave pump. *Lab Chip* 5:308–17
50. Ren H, Fair RB, Pollack MG. 2004. Automated on-chip droplet dispensing with volume control by electro-wetting actuation and capacitance metering. *Sens. Actuators B Chem.* 98:319–27
51. Shih SCC, Fobel R, Kumar P, Wheeler AR. 2011. A feedback control system for high-fidelity digital microfluidics. *Lab Chip* 11:535–40
52. Srinivasan V, Pamula VK, Fair RB. 2004. An integrated digital microfluidic lab-on-a-chip for clinical diagnostics on human physiological fluids. *Lab Chip* 4:310–15
53. Taniguchi T, Torii T, Higuchi T. 2002. Chemical reactions in microdroplets by electrostatic manipulation of droplets in liquid media. *Lab Chip* 2:19–23
54. Yoon JY, Garrell RL. 2003. Preventing biomolecular adsorption in electrowetting-based biofluidic chips. *Anal. Chem.* 75:5097–102
55. Yang H, Luk VN, Abelgawad M, Barbulovic-Nad I, Wheeer AR. 2009. A world-to-chip interface for digital microfluidics. *Anal. Chem.* 81:1061–67
56. Koc Y, de Mello AJ, McHale G, Newton MI, Roach P, Shirtcliffe NJ. 2008. Nano-scale superhydrophobicity: suppression of protein adsorption and promotion of flow-induced detachment. *Lab Chip* 8:582–86
57. Jonsson-Niedziolka M, Lapierre F, Coffinier Y, Parry SJ, Zoueshtiagh F, et al. 2011. EWOD driven cleaning of bioparticles on hydrophobic and superhydrophobic surfaces. *Lab Chip* 11:490–96
58. Luk VN, Mo G, Wheeler AR. 2008. Pluronic additives: a solution to sticky problems in digital microfluidics. *Langmuir* 24:6382–89
59. Au SH, Kumar P, Wheeler AR. 2011. A new angle on pluronic additives: advancing droplets and understanding in digital microfluidics. *Langmuir* 27:8586–94
60. Srinivasan V, Pamula VK, Fair RB. 2004. Droplet-based microfluidic lab-on-a-chip for glucose detection. *Anal. Chim. Acta* 507:145–50
61. Wijethunga PAL, Nanayakkara YS, Kunchala P, Armstrong DW, Moon H. 2011. On-chip drop-to-drop liquid microextraction coupled with real-time concentration monitoring technique. *Anal. Chem.* 83:1658–64
62. Lin L, Evans RD, Jokerst NM, Fair RB. 2008. Integrated optical sensor in a digital microfluidic platform. *IEEE Sens. J.* 8:628–35
63. Au SH, Shih SCC, Wheeler AR. 2011. Integrated microbioreactor for culture and analysis of bacteria, algae and yeast. *Biomed. Microdevices* 13:41–50
64. Barbulovic-Nad I, Yang H, Park PS, Wheeler AR. 2008. Digital microfluidics for cell-based assays. *Lab Chip* 8:519–26
65. Miller EM, Wheeler AR. 2008. A digital microfluidic approach to homogeneous enzyme assays. *Anal. Chem.* 80:1614–19
66. Luk VN, Wheeler AR. 2009. A digital microfluidic approach to proteomic sample processing. *Anal. Chem.* 81:4524–30
67. Miller EM, Ng AHC, Uddayasankar U, Wheeler AR. 2011. A digital microfluidic approach to heterogeneous immunoassays. *Anal. Bioanal. Chem.* 399:337–45
68. Dubois P, Marchand G, Fouillet Y, Berthier J, Douki T, et al. 2006. Ionic liquid droplet as e-microreactor. *Anal. Chem.* 78:4909–17
69. Poulos JL, Nelson WC, Jeon TJ, Kim CJ, Schmidt JJ. 2009. Electrowetting on dielectric-based microfluidics for integrated lipid bilayer formation and measurement. *Appl. Phys. Lett.* 95:013706
70. Karuwan C, Sukthang K, Wisitsoraat A, Phokharatkul D, Patthanasettakul V, et al. 2011. Electrochemical detection on electrowetting-on-dielectric digital microfluidic chip. *Talanta* 84:1384–89
71. Malic L, Veres T, Tabrizian M. 2009. Two-dimensional droplet-based surface plasmon resonance imaging using electrowetting-on-dielectric microfluidics. *Lab Chip* 9:473–75

72. Cho SK, Zhao Y, Kim CJ. 2007. Concentration and binary separation of micro particles for droplet-based digital microfluidics. *Lab Chip* 7:490–98
73. Zhao Y, Yi UC, Cho SK. 2007. Microparticle concentration and separation by traveling-wave dielectrophoresis (twDEP) for digital microfluidics. *J. Microelectromech. Syst.* 16:1472–81
74. Shah GJ, Ohta AT, Chiou EPY, Wu MC, Kim CJ. 2009. EWOD-driven droplet microfluidic device integrated with optoelectronic tweezers as an automated platform for cellular isolation and analysis. *Lab Chip* 9:1732–39
75. Mousa NA, Jebrail MJ, Yang H, Abdelgawad M, Metalnikov P, et al. 2009. Droplet-scale estrogen assays in breast tissue, blood, and serum. *Sci. Transl. Med.* 1:1ra2
76. Yang H, Mudrik JM, Jebrail MJ, Wheeler AR. 2011. A digital microfluidic method for in situ formation of porous polymer monoliths with application to solid-phase extraction. *Anal. Chem.* 83:3824–30
77. Abdelgawad M, Watson MWL, Wheeler AR. 2009. Hybrid microfluidics: a digital-to-channel interface for in-line sample processing and chemical separations. *Lab Chip* 9:1046–51
78. Watson MWL, Jebrail MJ, Wheeler AR. 2010. Multilayer hybrid microfluidics: a digital-to-channel interface for sample processing and separations. *Anal. Chem.* 82:6680–86
79. Jebrail MJ, Yang H, Mudrik JM, Lafreniere NM, McRoberts C, et al. 2011. A digital microfluidic method for dried blood spot analysis. *Lab Chip* 11:3218–24
80. Sista RS, Eckhardt AE, Wang T, Graham C, Rouse JL, et al. 2011. Digital microfluidic platform for multiplexing enzyme assays: implications for lysosomal storage disease screening in newborns. *Clin. Chem.* 57:1444–51
81. Sista R, Eckhardt AE, Wang T, Sellos-Moura M, Pamula VK. 2011. Rapid, single-step assay for Hunter syndrome in dried blood spots using digital microfluidics. *Clin. Chim. Acta* 412:1895–97
82. Cheng JT, Chen CL. 2010. Active thermal management of on-chip hot spots using EWOD-driven droplet microfluidics. *Exp. Fluids* 49:1349–57
83. Cheng JT, Chen CL. 2010. Adaptive chip cooling using electrowetting on coplanar control electrodes. *Nanoscale Microscale Thermophys. Eng.* 14:63–74
84. Paik PY, Pamula VK, Chakrabarty K. 2008. Adaptive cooling of integrated circuits using digital microfluidics. *IEEE Trans. Very Large Scale Integr. Syst.* 16:432–43
85. Paik PY, Chakrabarty K, Pamula VK. 2008. A digital-microfluidic approach to chip cooling. *IEEE Des. Test Comput.* 25:372–81
86. Baird E, Mohseni K. 2008. Digitized heat transfer: a new paradigm for thermal management of compact micro systems. *IEEE Trans. Compon. Packag. Technol.* 31:143–51
87. Mohseni K, Baird ES. 2007. Digitized heat transfer using electrowetting on dielectric. *Nanoscale Microscale Thermophys. Eng.* 11:99–108
88. Zhao Y, Chung SK, Yi UC, Cho SK. 2008. Droplet manipulation and microparticle sampling on perforated microfilter membranes. *J. Micromech. Microeng.* 18:025030
89. Zhao Y, Cho SK. 2006. Microparticle sampling by electrowetting-actuated droplet sweeping. *Lab Chip* 6:137–44
90. Moon I, Kim J. 2006. Using EWOD (electrowetting-on-dielectric) actuation in a micro conveyor system. *Sens. Actuators A Phys.* 130–131:537–44
91. Kuehne AJC, Gather MC, Eydelnant IA, Yun SH, Weitz DA, Wheeler AR. 2011. A switchable digital microfluidic droplet dye-laser. *Lab Chip* 11:3716–19
92. Fair RB, Khlystov A, Tailor TD, Ivanov V, Evans RD, et al. 2007. Chemical and biological applications of digital-microfluidic devices. *IEEE Des. Test Comput.* 24:10–24
93. Ito T, Torii T, Higuchi T. 2003. *Electrostatic micromanipulation of bubbles for microreactor applications*. Presented at IEEE Annu. Int. Conf. Micro Electro Mech. Syst., 16th, Kyoto, Jpn.
94. Pamula VK, Srinivasan V, Chakrapani H, Fair RB, Toone EJ, 2005. A droplet-based lab-on-a-chip for colorimetric detection of nitroaromatic explosives. *MEMS Miami: Tech. Dig.*, pp. 722–25
95. Vergauwe N, Witters D, Atalay YT, Verbruggen B, Vermeir S, et al. 2011. Controlling droplet size variability of a digital lab-on-a-chip for improved bio-assay performance. *Microfluid. Nanofluid.* 11:25–34
96. Nichols KP, Gardeniers JGE. 2007. A digital microfluidic system for the investigation of pre-steady-state enzyme kinetics using rapid quenching with MALDI-TOF mass spectrometry. *Anal. Chem.* 79:8699–704

97. Millman JR, Bhatt KH, Prevo BG, Velev OD. 2005. Anisotropic particle synthesis in dielectrophoretically controlled microdroplet reactors. *Nat. Mater.* 4:98–102
98. Martin JG, Gupta M, Xu Y, Akella S, Liu J, et al. 2009. Toward an artificial Golgi: redesigning the biological activities of heparan sulfate on a digital microfluidic chip. *J. Am. Chem. Soc.* 131:11041–48
99. Jebrail MJ, Ng AHC, Rai V, Hili R, Yudin AK, Wheeler AR. 2010. Synchronized synthesis of peptide-based macrocycles by digital microfluidics. *Angew. Chem. Int. Ed.* 49:8625–29
100. Keng PY, Chen S, Ding H, Sadeghi S, Shah GJ, et al. 2012. Micro-chemical synthesis of molecular probes on an electronic microfluidic device. *Proc. Natl. Acad. Sci. USA* 109:690–95
101. Rastogi V, Velev OD. 2007. Development and evaluation of realistic microbioassays in freely suspended droplets on a chip. *Biomicrofluidics* 1:014107
102. Sista RS, Eckhardt AE, Srinivasan V, Pollack MG, Palanki S, Pamula VK. 2008. Heterogeneous immunoassays using magnetic beads on a digital microfluidic platform. *Lab Chip* 8:2188–96
103. Vergauwe N, Witters D, Ceyssens F, Vermeir S, Verbruggen B, et al. 2011. A versatile electrowetting-based digital microfluidic platform for quantitative homogeneous and heterogeneous bio-assays. *J. Micromech. Microeng.* 21:054026
104. Wulff-Burchfield E, Schell WA, Eckhardt AE, Pollack MG, Hua Z, et al. 2010. Microfluidic platform versus conventional real-time polymerase chain reaction for the detection of *Mycoplasma pneumoniae* in respiratory specimens. *Diagn. Microbiol. Infect. Dis.* 67:22–29
105. Liu YJ, Yao DJ, Lin HC, Chang WY, Chang HY. 2008. DNA ligation of ultramicro volume using an EWOD microfluidic system with coplanar electrodes. *J. Micromech. Microeng.* 18:045017
106. Lin HC, Liu YJ, Yao DJ. 2010. Core-shell droplets for parallel DNA ligation of an ultra-micro volume using an EWOD microfluidic system. *J. Assoc. Lab. Autom.* 15:210–15
107. Malic L, Veres T, Tabrizian M. 2009. Biochip functionalization using electrowetting-on-dielectric digital microfluidics for surface plasmon resonance imaging detection of DNA hybridization. *Biosens. Bioelectron.* 24:2218–24
108. Malic L, Veres T, Tabrizian M. 2011. Nanostructured digital microfluidics for enhanced surface plasmon resonance imaging. *Biosens. Bioelectron.* 26:2053–59
109. Chang YH, Lee GB, Huang FC, Chen YY, Lin JL. 2006. Integrated polymerase chain reaction chips utilizing digital microfluidics. *Biomed. Microdevices* 8:215–25
110. Hua Z, Rouse JL, Eckhardt AE, Srinivasan V, Pamula VK, et al. 2010. Multiplexed real-time polymerase chain reaction on a digital microfluidic platform. *Anal. Chem.* 82:2310–16
111. Welch ER, Lin YY, Madison A, Fair RB. 2011. Picoliter DNA sequencing chemistry on an electrowetting-based digital microfluidic platform. *Biotechnol. J.* 6:165–76
112. Wheeler AR, Moon H, Bird CA, Ogorzalek Loo RR, Kim CJ, et al. 2005. Digital microfluidics with in-line sample purification for proteomics analyses with MALDI-MS. *Anal. Chem.* 77:534–40
113. Wheeler AR, Moon H, Kim CJ, Loo JA, Garrell RL. 2004. Electrowetting-based microfluidics for analysis of peptides and proteins by matrix-assisted laser desorption/ionization mass spectrometry. *Anal. Chem.* 76:4833–38
114. Moon H, Wheeler AR, Garrell RL, Loo JA, Kim CJ. 2006. An integrated digital microfluidic chip for multiplexed proteomic sample preparation and analysis by MALDI-MS. *Lab Chip* 6:1213–19
115. Jebrail MJ, Wheeler AR. 2009. Digital microfluidic method for protein extraction by precipitation. *Anal. Chem.* 81:330–35
116. Chatterjee D, Ytterberg AJ, Son SU, Loo JA, Garrell RL. 2010. Integration of protein processing steps on a droplet microfluidics platform for MALDI-MS analysis. *Anal. Chem.* 82:2095–101
117. Nelson WC, Peng I, Lee G-A, Loo JA, Garrell RL, Kim CJ. 2010. Incubated protein reduction and digestion on an electrowetting-on-dielectric digital microfluidic chip for MALDI-MS. *Anal. Chem.* 82:9932–37
118. Fiddes LK, Luk VN, Au SH, Ng AHC, Luk VM, et al. 2012. Hydrogel discs for digital microfluidics. *Biomicrofluidics* 6:014112
119. Luk VN, Fiddes LK, Luk VM, Kumacheva E, Wheeler AR. 2012. Digital microfluidic hydrogel microreactors for proteomics. *Proteomics*. In press
120. Jebrail MJ, Luk VN, Shih SCC, Fobel R, Ng AHC, et al. 2009. Digital microfluidics for automated proteomic processing. *J. Vis. Exp.* 6:1603

121. Shah GJ, Kim CJ. 2009. Meniscus-assisted high-efficiency magnetic collection and separation for EWOD droplet microfluidics. *J. Microelectromech. Syst.* 18:363–75
122. Park S, Wijethunga PA, Moon H, Han B. 2011. On-chip characterization of cryoprotective agent mixtures using an EWOD-based digital microfluidic device. *Lab Chip* 11:2212–21
123. Fan SK, Huang PW, Wang TT, Peng YH. 2008. Cross-scale electric manipulations of cells and droplets by frequency-modulated dielectrophoresis and electrowetting. *Lab Chip* 8:1325–31
124. Shah GJ, Veale JL, Korin Y, Reed EF, Gritsch HA, Kim CJ. 2010. Specific binding and magnetic concentration of CD8+ T-lymphocytes on electrowetting-on-dielectric platform. *Biomicrofluidics* 4:044106
125. Barbulovic-Nad I, Au SH, Wheeler AR. 2010. A microfluidic platform for complete mammalian cell culture. *Lab Chip* 10:1536–42
126. Eydelnant IA, Uddayasankar U, Li B, Liao MW, Wheeler AR. 2012. Virtual microwells for digital microfluidic reagent dispensing and cell culture. *Lab Chip* 12:750–57
127. Srigunapalan S, Eydelnant IA, Simmons CA, Wheeler AR. 2012. A digital microfluidic platform for primary cell culture and analysis. *Lab Chip* 12:369–75
128. Bogojevic D, Chamberlain MD, Barbulovic-Nad I, Wheeler AR. 2012. A digital microfluidic method for multiplexed cell-based apoptosis assays. *Lab Chip* 12:627–34
129. Witters D, Vergauwe N, Vermeir S, Ceyssens F, Liekens S, et al. 2011. Biofunctionalization of electrowetting-on-dielectric digital microfluidic chips for miniaturized cell-based applications. *Lab Chip* 11:2790–94

Annual Review of
Analytical Chemistry

Volume 5, 2012

Contents